Journal of Coastal Research	21	4	784–796	West Palm Beach, Florida	July 2005

Residual Flow Structure at a Scour-hole in Bahia Blanca Estuary, Argentina

Jorge O. Pierini[†‡], Gerardo M.E. Perillo[†§], María E. Carbone[†], and Fabián M. Marini[†]

[†]Instituto Argentino de Oceanografía
Casilla de Correo 804
8000 Bahía Blanca
Argentina
jpierini@criba.edu.ar
perillo@criba.edu.ar
ecarbone@criba.edu.ar
fmarini@criba.edu.ar

[‡]Comisión de Investigaciones Científicas de la Provincia de Buenos Aires

[§]Departamento de Geología
Universidad Nacional del Sur
San Juan 670
8000 Bahía Blanca
Argentina

ABSTRACT

PIERINI, J.O.; PERILLO, G.M.E.; CARBONE, M.E., and MARINI, F.M., 2005. Residual flow structure at a scour-hole in Bahia Blanca Estuary, Argentina. *Journal of Coastal Research,* 21(4), 784–796. West Palm Beach (Florida), ISSN 0749-0208.

Two-dimensional data of mean and sediment flow collected at a natural confluence of channels in the inner Bahía Blanca Estuary are presented. We describe the two-dimensional flow field to assess the role of changes in bed morphology occurring during transport-effective events on the structure of flow at a confluence; and to examine how the flow structure varies with changes in the ratio of momentum flux. At each station, vertical profiles of velocity, salinity, temperature and suspended sediment were obtained during the whole tidal cycle and residual fluxes were obtained. Lagrangean flux is higher than possible fresh water input, denoting an extra output of water which is the flux over the tidal flats along the southern and northern coasts of the channel. The effect of the junction produces a distortion of the vertical profile flow and in the suspended sediment transport. The effect of the particular conformation of the system makes necessary for consider the lateral effect of the tidal flats in the circulation of the estuary which exerts a significant influence.

ADDITIONAL INDEX WORDS: *Residual flow, scour hole, channels, tidal flats, suspended sediment flux.*

INTRODUCTION

Fluid dynamics of channel confluences are complex as combining flows may undergo mutual deflection, rapid acceleration, flow separation and give rise to a wide range of secondary circulations. It has become clear that understanding the details of these complex flow fields lies at the heart of the interpretation of sediment transport pathways and development of bed morphology at junctions (ROY and DE SERRES, 1989; BEST and ROY, 1991).

The natural channels thalwegs of two confluent channels are discordant, then a tributary step gives rise to a lateral motion of fluid from the deeper channel towards the shallower tributary, and results in a distortion of the mixing layer between both flows. These effects can be of considerable importance for studies of transport, mixing and deposition of contaminated media. Most studies at river channel confluences have yielded better, yet still incomplete, understanding of the link between flow dynamics, sediment transport and bed morphology at these sites (MOSLEY, 1982; BEST, 1985, 1987).

At the confluence of two tributaries there are major changes in the bed geometry due to dynamical complexities that normally arise there. One of the most common morphological consequences is the development of scour holes. Studies of scour holes are concentrated at river confluences where their morphological features have been related to the angle of the junction, tributary discharge ratio and degree of sediment erodability (BEST, 1987).

Similar scour holes were found in tidal environments. However these features at tidal channel junctions have received little attention as there are only two articles in literature describing their geomorphology and general circulation pattern (KJERFVE *et al.,* 1978; GINSBERG and PERILLO, 1999). In the marine environment the unsteady behavior of the dominant processes, like tides, winds or waves, and the periodical changes in current direction may induce further complexity on the formation and evolution of the features that may not be readily observed in unidirectional flows. For instance, recently WARNER *et al.* (2002) have described changes from dominant barotropic to gravitational to baroclinic circulation at the junction of two straits in San Francisco Bay associated to various river discharge situations.

The aim of this paper is to provide a description of the vertical structure in the transport of water, salt and suspended sediment at a channel confluence having a scour hole. In this case, the tributary also is a source of freshwater. We describe the two-dimensional flow field to assess the role of

DOI: 10.2112/010-NIS.1 received and accepted in revision 8 March 2004.

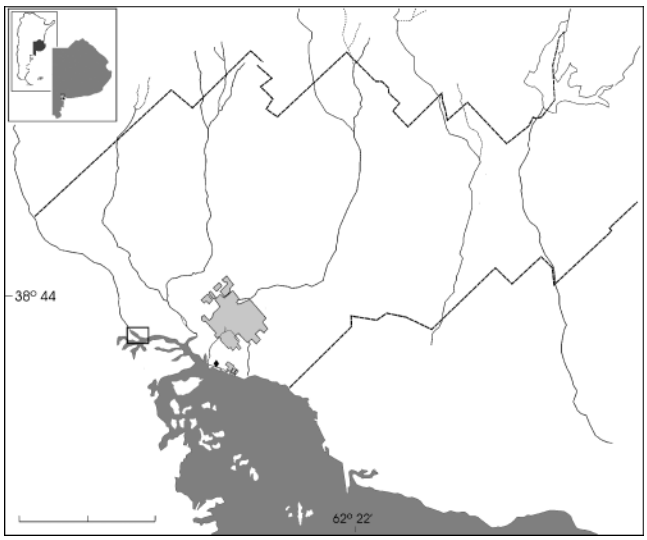

Figure 1. Location map of Bahia Blanca Estuary and base station.

change in bed morphology occurring during transport-effective events on the structure of flow at the scour hole and to examine how the flow structure varies with changes in the ratio of momentum flux.

The study concentrates on the inner reach of the Bahía Blanca Estuary (Argentina; Figure 1). The general geomorphologic and dynamic features of the estuary have been described elsewhere (*e.g.,* PICCOLO and PERILLO, 1990; PERILLO and PICCOLO, 1991, 1999). At this site, a branch of the Sauce Chico River, major source of freshwater for the estuary, joins the Canal Principal with an angle of 55°, which is only slightly lower than those values estimated for very large holes observed somewhere in the estuary (GINSBERG, 1993). Also, it is the only scour hole with freshwater discharge into the inner estuary.

MATERIALS AND METHODS

To determine the general geomorphologic and oceanographic conditions at the confluence, a bathymetric survey, bottom sediment sampling and water column data were gathered on 7 and 8 September 1998. A detailed bathymetry survey was made during high tide. Data were gathered in profiles across the channel every 50 m plus two controllery longitudinal profiles. Depth data was obtained employing a Raytheon 208 kHz echosounder and the vessel positioned by a differential global positioning system (DGPS). Bathymetric data was post processed and correct to the Datum Plane for the area using information from a tidal gauge operated by the Dirección Nacional de Construcciones Portuarias y Vias Navegables (DNCPVN; Figure 3) less than 5 km from study site.

Physical measurements were made in a cross-section perpendicular to the channel over the confluence (Figure 1) at three stations (C1, C2, C3) positioned in order to cover the most important morphological features of the section. A bathymetric profile was made using the echo sounder and the stations were fixed with anchors and buoys, previously positioned by DGPS (Figure 2). Data was obtained for over a tidal cycle (13 h) starting before and ending after a high tide. Tidal cycle corresponded to middle conditions between spring and neap stages so the data represents the average situation for the site.

The field methodology employed was originally designed by PERILLO and PICCOLO (1993) to study an estuarine cross section using only one boat and one set of instruments. A summary of the general procedure is given as follows. Each station is occupied alternatively in a cycle 1,2,3,2,1, for the entire measurement period. Following this procedure, C2 is sampled almost twice as much as the other stations, thus providing a much better view of the time evolution of the parameters. At each station, vertical profiles of velocity, salinity, temperature and suspended sediment were obtained. Speed and direction of currents were measured using a current meter Valeport BMF 108. Conductivity and temperature were measured using a Mini CTD Interocean, and suspended sediments with an Optical Backscatter Sensor (OBS) attached to the CTD. Sea level was registered at the tidal gauge indicated previously.

Reduction of the data also followed the procedure developed by PERILLO and PICCOLO (1993) to convert data sampled at irregular time and space intervals in a pseudo synoptic data array. First, current vectors were discomposed into a component parallel to the axis of the estuary (U) at the cross section, and another transversal (V) to it. With this correction, component flowing in the ebb direction and to the right, respectively, were considered positive (Figure 2).

Data at five non dimensional levels 0.1 (0.2) . . . 0.9 and at 1 hour intervals (Δt) were obtained by interpolation using the Stineman algorithm (PERILLO and PICCOLO, 1991) After the reduction, a three-dimensional matrix containing seven rows by five columns with 13 time steps are formed for each variable. To obtain the fluxes of water (Q), salt (F) and suspended sediment concentration (P) data were further interpolated to a proportional grid with equal-area cells proposed by PERILLO and PICCOLO (1998). Integration over the total cycle gave the net flow of the variables mentioned following the averaging method presented by KJERFVE (1979).

Estimation of Residual Fluxes

Determination of residual fluxes through an estuarine cross-section requires a specific procedure to avoid errors produced by the method which are of the same order of the expected results. Different authors have estimated them without paying enough attention to the grid design. This was first suggested by RATTRAY and DWORSKI (1980). PERILLO and PICCOLO (1998) have demonstrated that the proportional grid is the only one which does not introduce spurious errors. Therefore, values calculated here will follow their procedure, which will be briefly described.

The cross-section area for each time step was divided into 35 cells of equal size, each represented by a data point interpolated at a seven levels or rows (i) and five columns (j) defined by the number of stations occupied plus two. Each cell

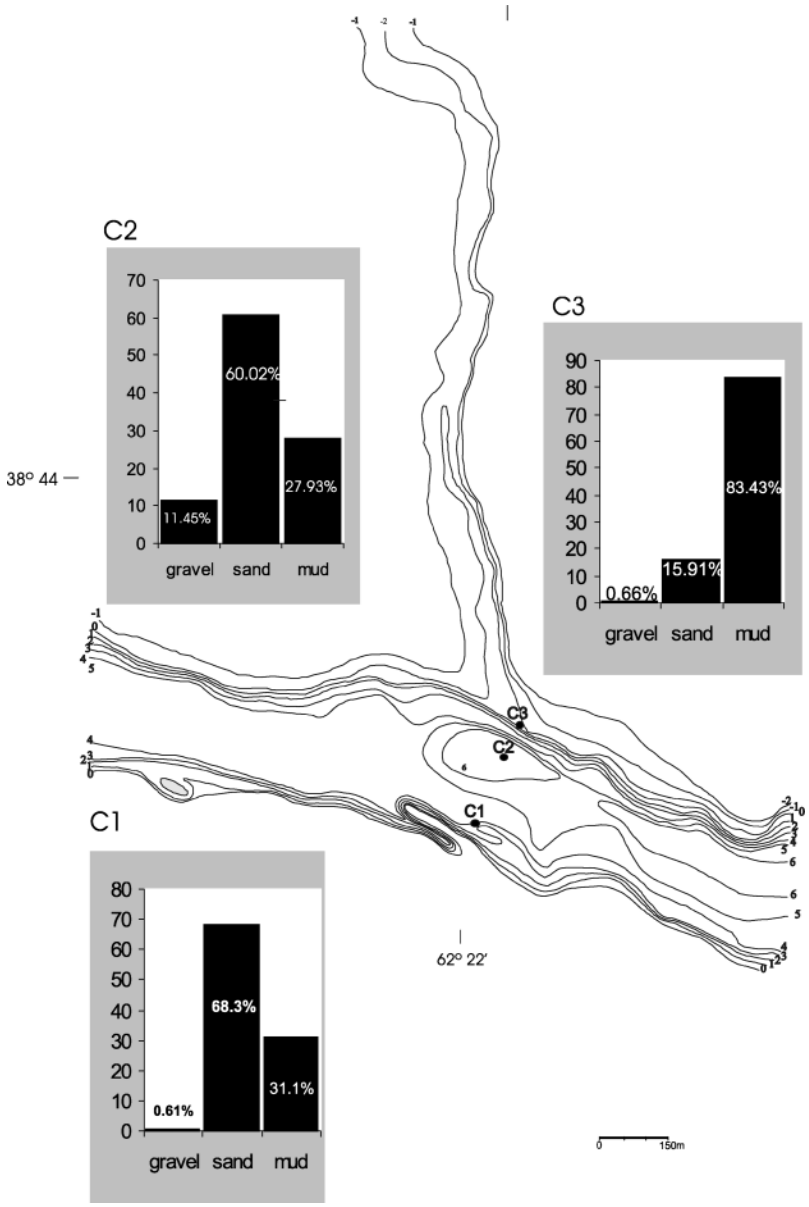

Figure 2. Bathymetric chart of the Sauce Chico River and granulometric distribution over each station.

has a time-varying area (A_{ijk}), and at the center of each cell, for every $\Delta t = 1$ h, the values of the longitudinal component of the velocity (U_{ijk}), salinity (S_{ijk}) and suspended sediment concentration (C_{ijk}) were interpolated at the center of each grid cell for each time k.

The instantaneous rates of transport of water (Q), salt (F) and suspended sediment concentration (P) through each cell element are calculated using;

$$Q_{ijk} = \rho A_{ijk} U_{ijk} \quad (1)$$

$$F_{ijk} = S_{ijk} Q_{ijk} \quad (2)$$

$$P_{ijk} = C_{ijk} Q_{ijk} \quad (3)$$

Based on these parameters, a series of residual fluxes may be calculated, and the relation for the residual transport of salt and suspended load averaged over the tidal cycle can be estimated by integrating the areas over the section and time,

$$\langle F_{vt} \rangle = \langle F_l \rangle + \langle F_{tp} \rangle + \langle F_{vs} \rangle + \langle F_{st} \rangle + \langle F^* \rangle \quad (4)$$

$$\langle P_{vt} \rangle = \langle P_l \rangle + \langle P_{tp} \rangle + \langle P_{vs} \rangle + \langle P_{st} \rangle + \langle P^* \rangle \quad (5)$$

Diamond brackets stand for an average over a tidal cycle. Whereas the terms with subscript *l* are the rate of transport due to the Lagrangean residual flow over the section; those with subscript *tp* are the rate of transport due to tidal pumping, the ones with subscript *vs* are due to vertical shear dis-

persion; while the subscript *st* indicates the residual transport due to the transverse shear dispersion. Finally, the terms with superscript * are introduced by the interaction between vertical and transversal deviations from the mean cross-sectional averages.

On the other hand, the residual transport of water can be written (UNCLES *et al.,* 1985)

$$\langle Q_{vt} \rangle = \langle Q_s \rangle + \langle Q_e \rangle \quad (6)$$

where

$$\langle Q_s \rangle = \langle A \rangle \langle \bar{U}_s \rangle \quad (7)$$

$$\langle Q_e \rangle = \langle A \rangle \langle \bar{U}_e \rangle \quad (8)$$

$$\langle Q_{vt} \rangle = \langle A \rangle \langle \bar{U}_l \rangle \quad (9)$$

Variable $\langle A \rangle$ is the tidal averaged cross-sectional area, $\langle \bar{U}_s \rangle$ is the mass transport produced by the Stokes drift; $\langle \bar{U}_e \rangle$ is the Eulerian residual current averaged over the section, and $\langle \bar{U}_l \rangle$ is the sectional averaged mass (water) transport residual current, also known as Lagrangean residual current.

RESULTS AND DISCUSSION

The morphology and sedimentology of the inner reach of the Canal Principal was originally described by GÓMEZ *et al.* (1997). We describe in detail only the specific sector of interest (Figure 2) which corresponds to 1200 m along the Canal Principal with a general WNW-ESE orientation (106°). At about the middle point of the study area, the Sauce Chico River having a general trend N-S, joins the channel with an angle of 55°. The Canal Principal varies in width (considering the boundary at the Datum Plane) between 150 and 250 m, although in high tide may reach widths of the order of 500 m. Maximum depth in the Canal Principal is found at the scour hole with 6.7 m, but average depth is on the order of 5 m. The bottom is relatively flat but the channel borders are rather steep as they were cut through the very compact former delta sediments, becoming a tidal flat when moving above the −1 m isobath (negative depths are values above Datum Plane).

On the other hand, the final reach of the Sauce Chico River corresponds to a very shallow channel. At low tide, it appears as a narrow channel about 10–15 m wide with depths of the order of 1 m or less. The depth ratio (depth of tributary/depth of main channel) ranges from 0.36 at low tide to 0.63 at high tide.

Morphologically, the scour hole is similar to others found at various junctions in the Bahía Blanca Estuary. It has an upside-down truncated cone shape with an ellipsoidal section (Figure 2). The bottom is relatively flat between 6 and 6.7 m deep. Contrary to scour holes found in rivers, the upstream flank is steeper than the downstream one. Although also contrary to the other holes observed in the estuary, the hole is completely contained within the Canal Principal and does not have a minor incision into the tributary as it occurs at the other holes in the estuary. (GINSBERG and PERILLO, 1999).

Bottom sediments taken at the three stations clearly represents the different hydrodynamic conditions that the study area is subjected. Both samples taken in the Canal Principal (C1 and C2) are silty sands (Figure 2). Median values for these samples (D_{50}) are 2.79 ϕ and 3.17 ϕ, respectively. The main difference between them is the percentage of gravel size material found at the scour hole. On the other hand, the mud/sand concentrations are fully reversed in the sample taken at the mouth of the Sauce Chico River (C3, median = 6.07 ϕ). Energetic conditions within the river are only important during high river discharge and during max ebb which justifies the fine sediments found there. Also the river provides very little sand due to the controls that it has upstream.

During the study period, wind blew from WSW sector with average speed of the order of 10 m s^{-1} (Figure 3). This direction has relatively little effect over the circulation at the reach even with high tide as the channel is bounded by an island on that direction. Therefore, all processes determined during this study correspond only to the interaction of the tidal wave and freshwater input over the geomorphology. Tidal range was 3.55 m. during the physical measurements.

Depth-time series for salinity, temperature and suspended sediment concentration for the whole tidal cycle at each station are shown in Figures 4 (C1), 5 (C2) and 6 (C3), respectively. Although Station C3 was located at the thalweg of the tributary channel, during over 6 h around low tide, water depth was to low to allow the vessel to reach it, thus this period appears blank in the figure. Salinity and temperature fluctuated between 26.6 and 28.6 and between 11.8 and 12.4° C, respectively, at all stations.

Salinity profiles are nearly vertical having as much as 2 of salinity stratification indicating a high degree of vertical mixing and with only minimum stratification near low tide (Figure 4a; 5a and 6a). However, salinity values are relatively low for the reach and period. Normal salinity values are around 30 reaching maxima of over 36 (PERILLO *et al.,* 1987). Precipitations in the drainage basin in year 1998 were over the average which produced a larger input than normal of freshwater into the system. Similar conditions are observed for temperature (Figure 4b; 5b and 6b), although it is clear that it increased along the day due to solar radiation. The tidal cycle was measured at the end of the winter so water temperatures are about normal for the period.

Suspended sediment concentration varied from 20 to 105 mg l^{-1} along the whole tidal cycle (Figure 4c; 5c; 6c), being normal for the reach. The highest concentration was observed over the scour hole at C2 during the flood. Even though most profiles are vertically homogeneous, maximum values appear near the bottom, specially at stations C1 and C2, coincident with the maximum velocities. Thus, these peak concentrations can be considered as processes of resuspension of bottom sediments. Maximum longitudinal speed was 0.36 m s^{-1} for flood and 0.72 m s^{-1} for ebb at the surface and mid-depth, respectively (Figure 7a). Bottom velocities were relatively small, especially in the station C1 and during flood.

To illustrate the temporal occurrence of mixing at the stations, the relative contributions of the density gradient and the velocity shear to the Bulk Richardson Number (Ri) throughout the tidal period mixing diagrams following DYER and NEW (1986) for stations C1 and C2 were made (Figure 8). In a mixing diagram the surface-to-bottom salinity difference (Δs) is plotted against $\bar{U}|\bar{U}|$. According with the specified

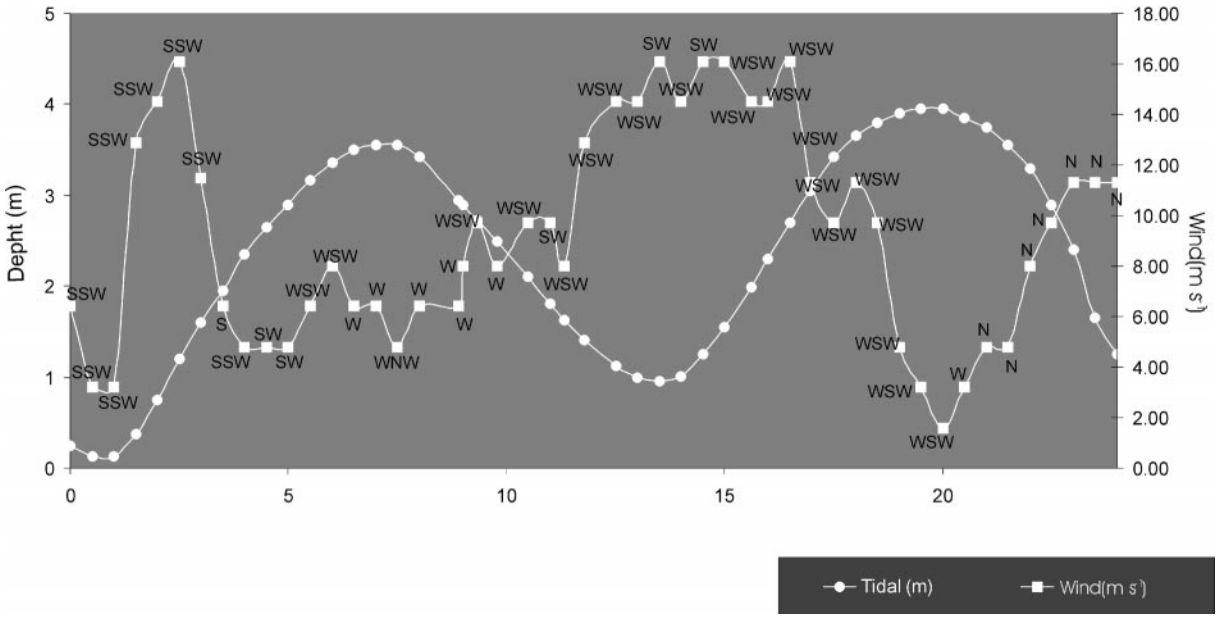

Figure 3. Tidal wave in base station and wind distribution (magnitude and direction).

coordinates $\tilde{U}|\tilde{U}| < 0$ represents flood conditions. The limits of Ri $<$ 2 and 20 are presented for the appropriate water depth, assuming that the salinity stratification is directly proportional to the density stratification

Mixing (2 $<$ Ri $<$ 20) and well-developed mixing (Ri $<$ 2) occurred all the time in the cross section, being strongest when the currents reached maximum intensity on the flood or ebb tides. Most of the ebb and flood oriented fluxes are concentrated in the deepest part of the channel over the center station (Figure 8b). At the two stations considered, stratification increased during the ebb tide, which suggests that the bottom shear failed to mix the more stratified water being advected from upstream. Near slack water, stratification was markedly reduced, indicating advection of well-mixed water from upstream.

Cross-sectional residual fluxes are estimated by time-averaging the salt and suspended sediment fluxes in each individual cell. Due to the proportional grid used, each cell has equal area; therefore, the variance is equally distributed all over the section making it error-free with regard to the calculation method. Both fluxes clearly show a center core of ebb oriented residual transport with maximum values at the surface (Figure 9a,b). Headward fluxes appear along the borders and at the bottom of the center portion of the channel. Thus, this sector alone appears as having a partially-mixed vertical structure but defined by the residual currents rather than the salinity distribution. This type of vertical residual flux structure is common along the northern flank of the Canal Principal at other cross-sections (PICCOLO and PERILLO, 1990; PÉREZ and PERILLO, 1998). Similarly the southern portion having a headward residual flux for the full water column has also been observed at various places along the estuary and it was assigned to the effect of the large southern tidal flats on the circulation (PERILLO *et al.,* 2002).

Two mechanisms can redistribute salt laterally in estuaries. Large axial density gradients can force a secondary (cross-channel) circulation that converges to form an axial front (NUNES and SIMPSON, 1985). Convergent flow into axial fronts during flood redistributes momentum downward and reverses the vertical shear in the flood current. This induces a subsurface maximum in the current field (TURRELL *et al.,* 1996). Salt trapping provides a second mechanism (FISCHER *et al.,* 1979) where phase differences of salt transport in connecting channels alters the distribution of salt (OKUBO, 1973).

While we cautiously interpret subsurface flow features from measurements at three points, some high water and low water current measurements indicate the presence of subsurface high velocity cores during some part of the flood flow. Flood and ebb tidal current asymmetries in the main and small side channels play an equally important role in the lateral redistribution of salt. Salt is redistributed by changes in the relative phase of salt transport between adjacent channels. Since the upper portion of the water column at Station C2 ebbs for an additional hour after flood currents begin in the lower and southern portions of the Canal Principal, a small volume of low salinity water flows seaward on the north side. This water mass is inserted into the Canal Principal where it mixes with the flood currents transporting a larger volume of sea water landward on the south side.

Also, a possible reason for the large flood oriented residual fluxes at the northern portion results in the fact that we were notable to measure during part of the ebb because water depth did not allow to reach Station C3 with the boat. Al-

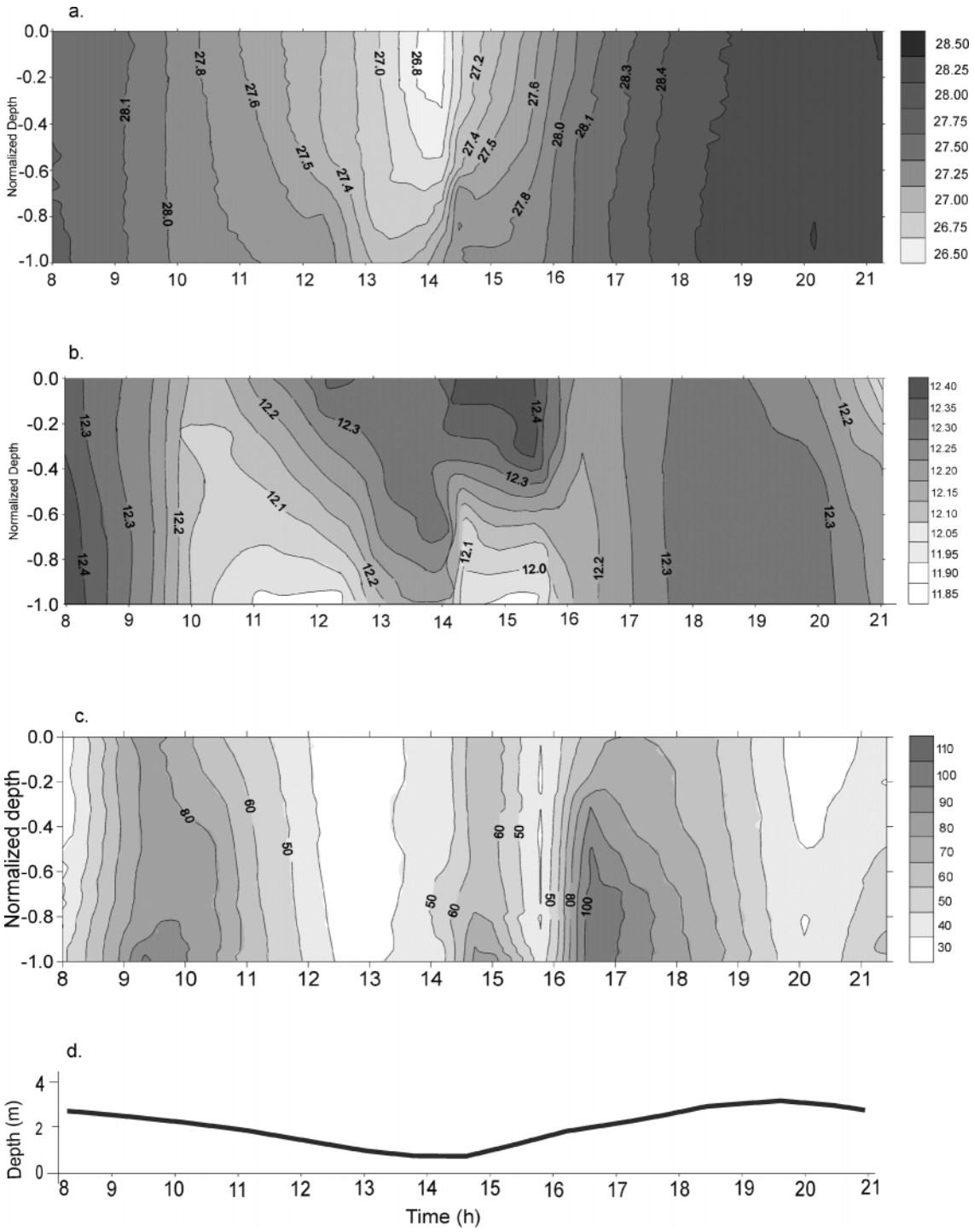

Figure 4. Vertical distribution of salinity (a), temperature (b) and suspended sediment (c) and tidal wave (d) at the south station (C1).

though, the low river discharge may not have produced a large difference in the estimated value. When correlated the center of the flood oriented cells of residual salt and suspended sediment fluxes on the northern side (Figure 9), they coincide with the tributary channel.

The sea water which floods into the estuary in the Canal Principal during the initial flood period is diluted with a small amount of low salinity estuarine water still streaming seaward in the tributary. Since ebb transport at Station C2 carries much larger volumes of low salinity water, a large,

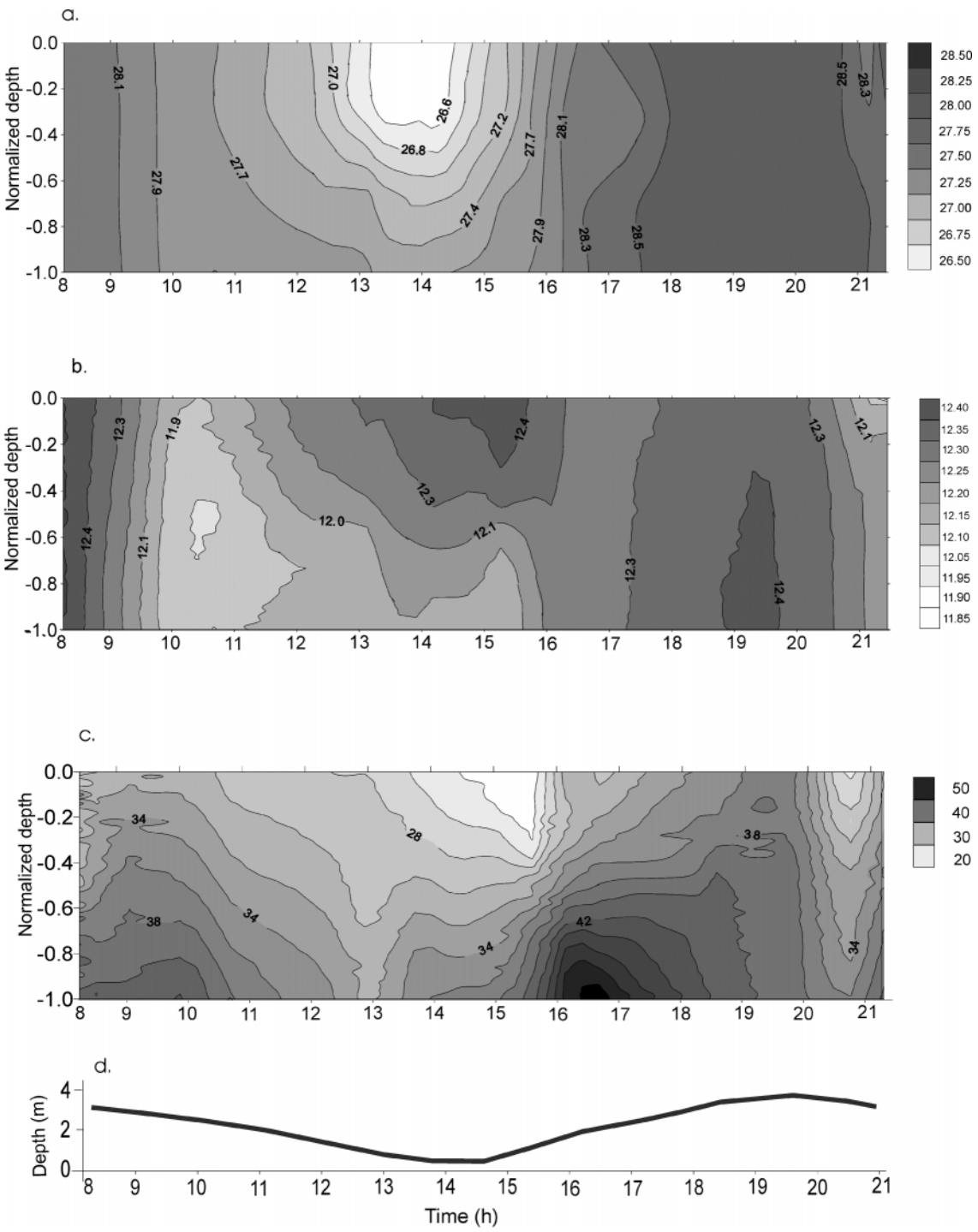

Figure 5. Vertical distribution of salinity (a), temperature (b) and suspended sediment (c) and tidal wave (d) at the center station (C2).

easily traced source of low salinity water is formed at low water slack downstream at the mouth of the small side channel at Station C3 and Sauce Chico River runoff. This water is subsequently advected in with the flood tide and is the origin of the low salinity water observed during the first part of flood. As water level continues to rise, low salinity water from the main channel is eventually replaced by higher salinity water flooding into the estuary, as shown in the salt residual fluxes (Figure 9a). After high water slack, ebb flows initially introduce lower salinity water from upstream into

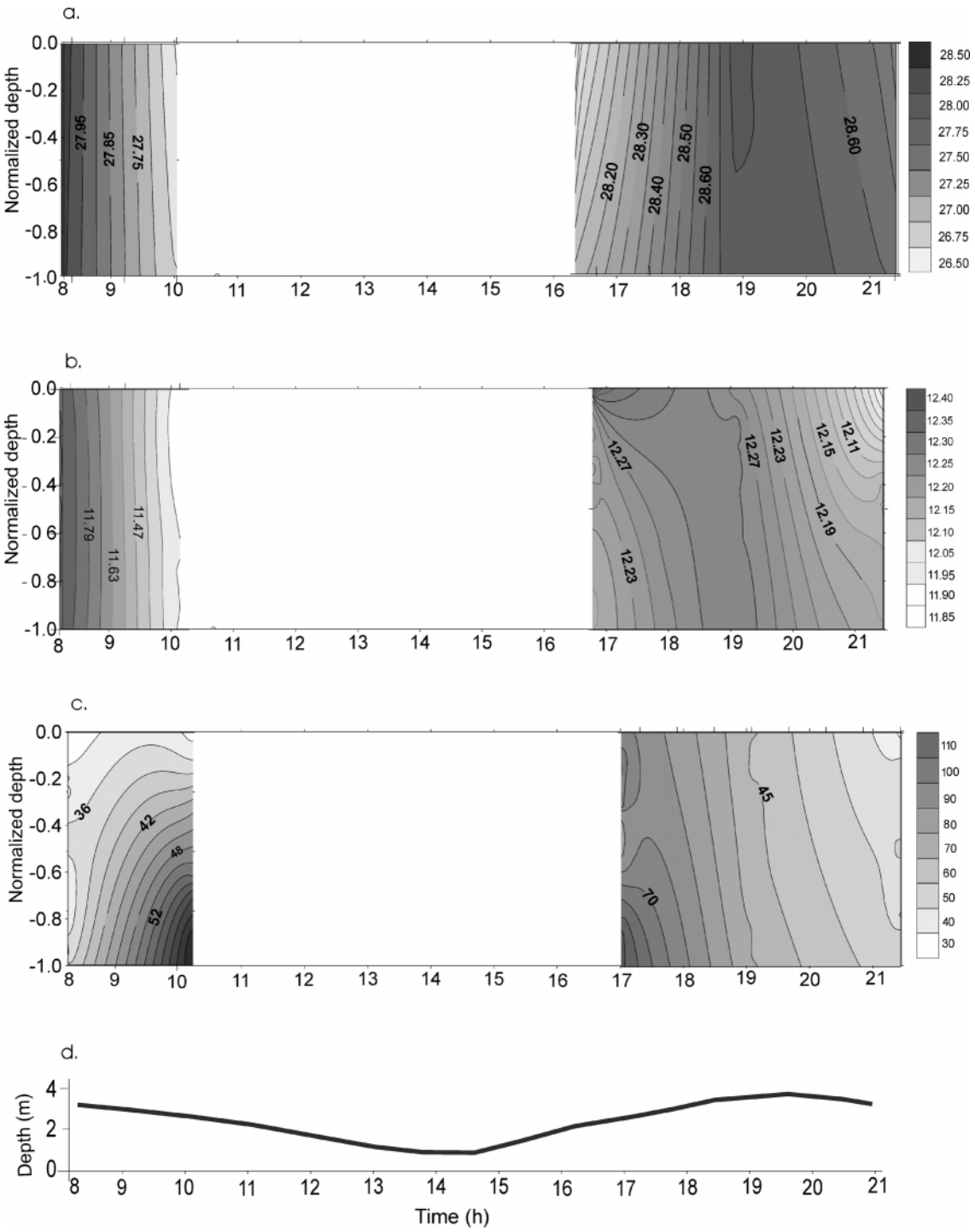

Figure 6. Vertical distribution of salinity (a), temperature (b) and suspended sediment (c) and tidal wave (d) at the north station (C3).

the channel at Station C1. As water level continues to fall, the salinity ceases to decrease. Thus the flood dominance limits the amount of low salinity water that can flow through this channel. On the other hand, the residual fluxes are not affected by the presence of the hole.

The Lagrangean, Eulerian and Stokes fluxes are given in Table 1. The Stokes transport that is produced by the progressive nature of the tidal wave is small, demonstrating that the inner estuary has a relatively high frictional capability. Although the Eulerian transport represents a balance to the

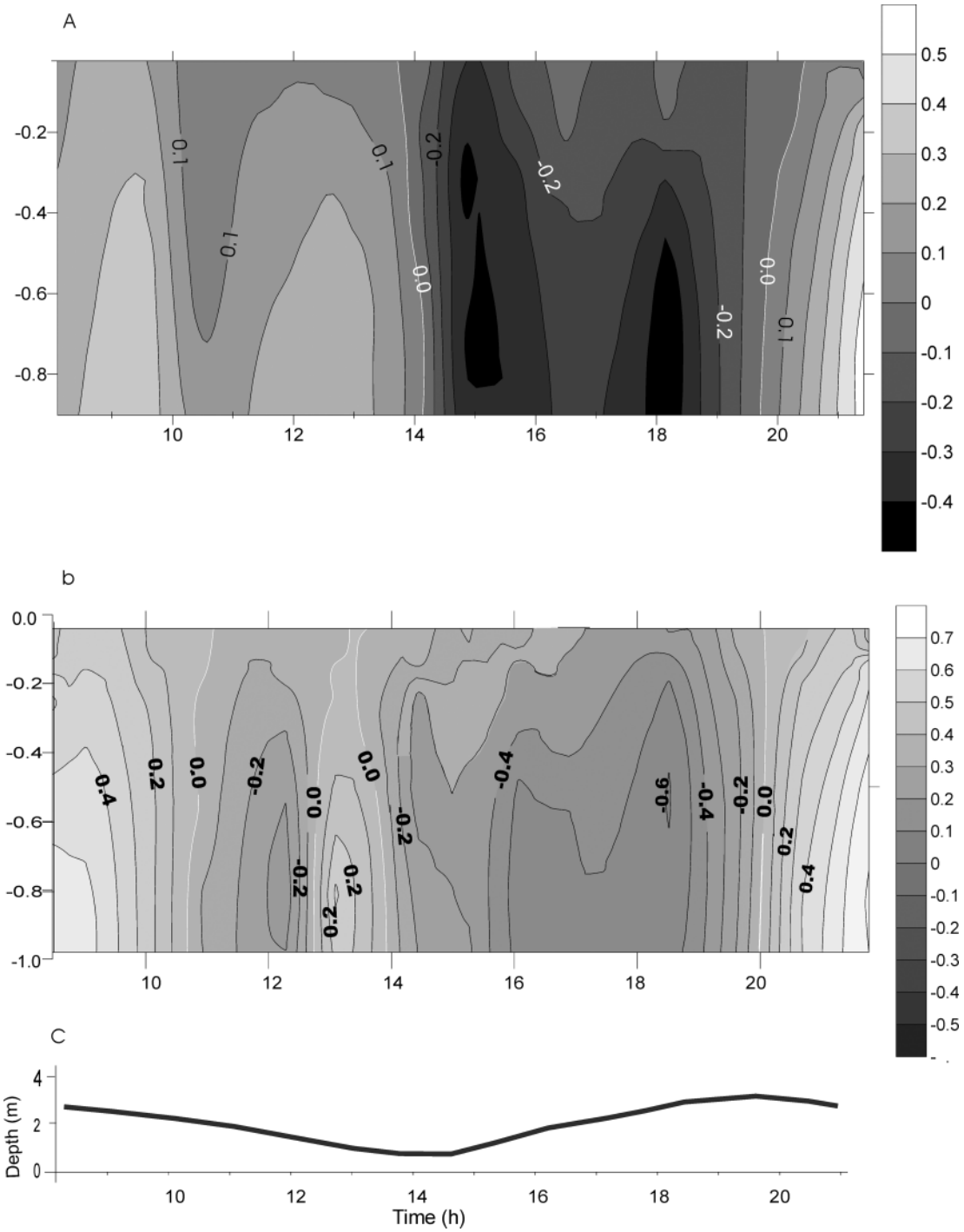

Figure 7. Longitudinal velocities distribution over south (a) and center (b) station. Tidal wave (c).

Stokes pumping and should be positive as well as the Lagrangean term for a standard, well-behaved estuary. In the present case, the effect of the southern tidal flats and the flood-dominated results coming from the tributary data, induces a negative result for the Eulerian transport, suggesting that water is being stored in the estuary. However, because a non-defined percentage of the water bypass the cross-section on the lateral flats during ebb, the system is actually balanced.

Residual fluxes of salt (F) and suspended sediments (P)

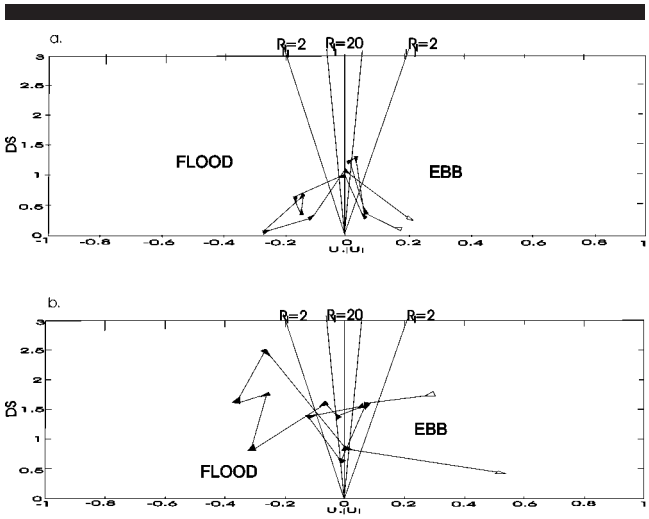

Figure 8. Mixing diagram at the south (a) and center (b) station measured.

were estimated for the cross-section employing equations (4) and (5) (Table 2). The total residual rate of transport of both salt and suspended sediments are directed down-estuary driven mainly by the total shear ($Y_s = Y_{vs} + Y_{st} + Y^*$, Y is used as a generic variable). Thus, these processes were advective. Being these values much larger than the tidal pumping (Y_{tp}) and of the same order than the Lagrangean (Y_l) but of different sign, emphasizes their importance in a tidal dominated estuary. From the three shear values, the transversal one was by far the largest, specially in the case of the suspended sediments. Contrary to what was found by UNCLES *et al.* (1985), the results obtained here have larger transversal shear than vertical, but also, the transversal shear in the present cross-section was comparatively smaller than that obtained by PEREZ and PERILLO (1998) in a cross-section of the Bahía Blanca Estuary at least twice as wide.

Both the Lagrangean and tidal pumping terms have signs reversed than expected from the theory. In the later case, there are examples (UNCLES *et al.,* 1985) where positive tidal pumping was also found and assigned to the effect of the friction induced by the shallower portions of the cross-section. On the other hand, a negative Lagrangean flux is indicating that water is being imported into the estuary at much larger rate than the exportation of freshwater. For the study area, freshwater output is very small, about 2 $m^3\ s^{-1}$ considering total discharge of the Sauce Chico River from the main outlet (located 4 km upstream of the cross-section) and the output at the study site. This volume is small to compensate the volumes that return seaward on top of the tidal flats and cannot be accounted by the measurement methodology, resulting a fictitious headward flux.

The general characteristics of the mean flow field at the confluence described in this paper must be related to an understanding of the morphological characteristics of the site and the changes through the study period. This site is representative of many confluences of discordant beds in that

Table 1. *Residual fluxes and velocities for water mass.*

Fluxes	Lagrangean	Eulerian	Stokes
<Q> (m^3/s)	−7.14	−6.50	−0.64
<U> (m/s)	−0.11	−0.10	−0.01

the morphology of the beds is not dominated by a pronounced scour. The typical morphology of the bed at the site consists of a local scour that is evident as a gentle depression bounded by the 6 m isobath (Figure 2). Deep scour holes on tidal channels differ from their river counterparts because they have the steeper side pointing into the tributaries and the gentler away from them, whereas in rivers the sides are reversed (GINSBERG and PERILLO, 1999).

In the present case, the inner deeper areas show an extended dune field conformed by shelly sandy sediments. These features have a mean wavelength of 4 m, which according to ASHLEY (1990) could be classified as 2D and 3D median dunes. In the inner sector the dune field is attributed to ebb currents increasing along the channel.

The flow structure at this confluence of discordant-bed channels was examined in relation to the current vectors. Velocity vector distributions at the three stations for various significant stages of the tide (Figure 10) show a difference in the magnitude of the near-bed and near surface values. The vectors over the avalanche face present an apparent flow deflection as the fluid enters the junction. Near-bed flows show some differences in magnitude from those near the surface, with the near-surface flow experiencing less deflection at that point. The difference in magnitude with height above the bed is most pronounced near the avalanche face and is linked to the difference in height between the two channels.

At the confluence the morphology of the bed and flow patterns, vary with changes in the tide conditions. BEST and REID (1984) analyzed this situation employing the discharge ratio (Q_S/Q_M) since the depth and width of the wetted perimeter are not constant. We introduce here the estimation of the momentum flux ratio defined as:

$$M_f = \frac{\rho_C U_C Q_C}{\rho_M U_M Q_M}$$

where Q is the discharge ($m^3\ s^{-1}$), U is the velocity ($m\ s^{-1}$), ρ is the water density ($kg\ m^{-3}$) and subscripts C and M refer to the cell and mean flow, respectively. This parameter defines the influence of each cell normalized by the mean total momentum flux for the cross-section. Therefore, the results illustrate the net transport of momentum which is dominant in the lower part of the channel at both sides of the scour

Table 2. *Estimated residual fluxes for salt (F) and suspended sediments (P) as described in eqs. (4) and (5). Y is a dummy variable representing either F or P.*

Fluxes	Y_{vt}	Y_l	Y_{tp}	Y_{vs}	Y_{st}	Y*	Y_S
F (salt)	76.32	−86.16	13.76	52.67	96.09	−0.04	148.72
P (SS)	39.80	−155.07	1.22	65.21	218.58	−90.15	193.64

F units: (Salinity units $.m^3\ s^{-1}$)
P units: ($mg\ l^{-1}\ .\ m^3\ s^{-1}$)

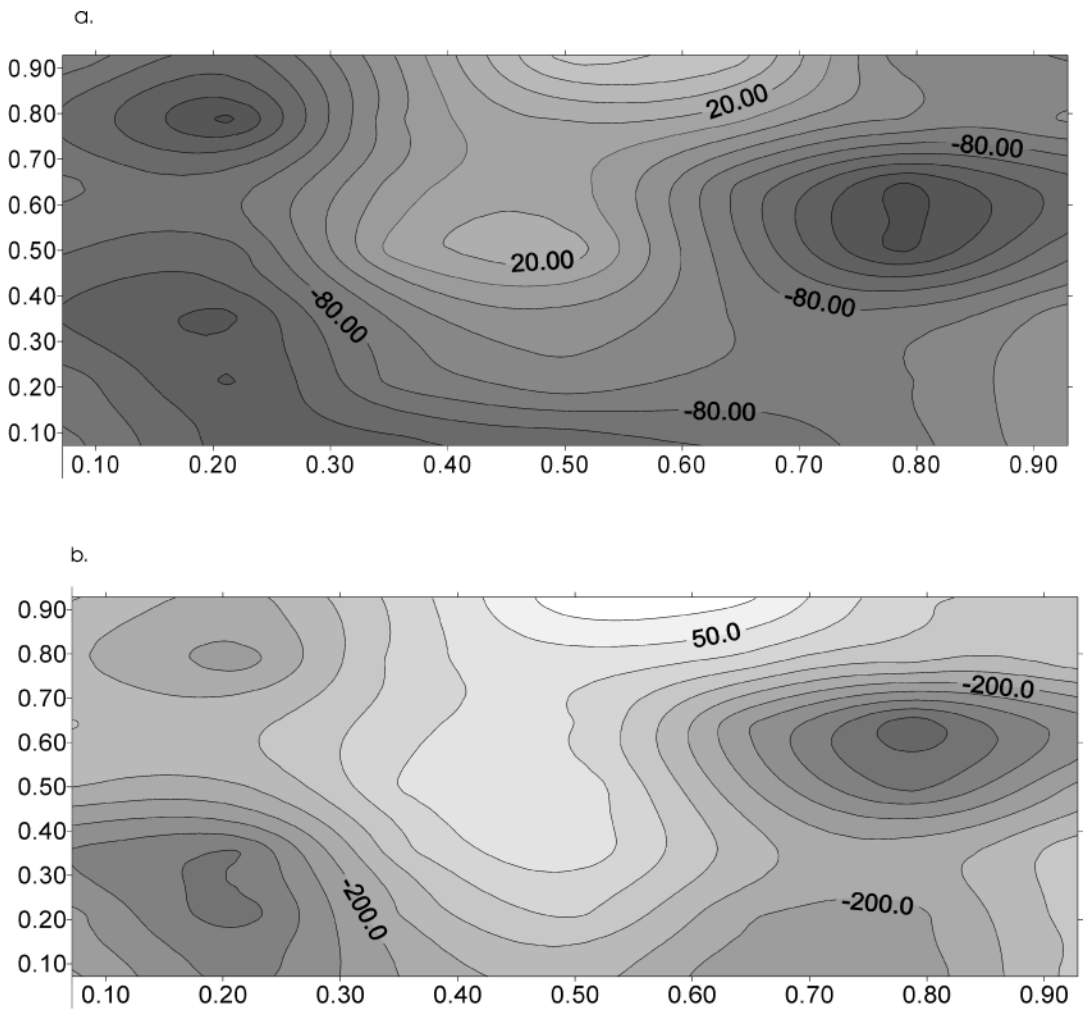

Figure 9. Residual salt (a) and suspended sediment (b) fluxes at normalized cross section.

hole (Figure 11). At the scour hole proper, there is a minimum momentum flux, as if the sudden increase in depth may induce a relaxation of the flow. The net acceleration along the northern border of the hole may be induced by the avalanche face.

CONCLUSIONS

The circulation and dynamics along a tidal cycle have been analyzed in one of the innermost areas of the Bahía Blanca Estuary having a channel junction which is a common feature in the estuary. Data demonstrated that the cross section behaves as partly mixed but based only on the residual current vertical structure. Salinity, temperature and suspended sediment profiles are nearly vertical homogeneous and with only minimum stratification during low tide conditions.

When the residual fluxes where decomposed, the Lagrangean flux appears higher than possible freshwater input. Although river discharge was not determined, averages values do not coincide with the estimated values, denoting an extra output of water over the tidal flats along the southern and northern coasts of the channel. Due to the presence of the flats and the logistic difficulties measuring the circulation on top of them, becomes impossible to control continuity in the system.

Although the scour hole seems to be an important geomorphological feature at the cross-section, it did not produced major modifications in the circulation except when it was analyzed based on the momentum flux approach. In this analysis, it is clear that the sudden change in depth at the hole produces a relaxation in the momentum flux which becomes concentrated along both sides of the hole. This is particularly notable when the northern peak of momentum flux is associated with the tributary channel.

The effect of the tidal flats in this type of estuaries, where water not necessarily returns with the same input pattern, must be considered further. The main difficulty is to be able to measure the circulation simultaneously with restricted instrumentation.

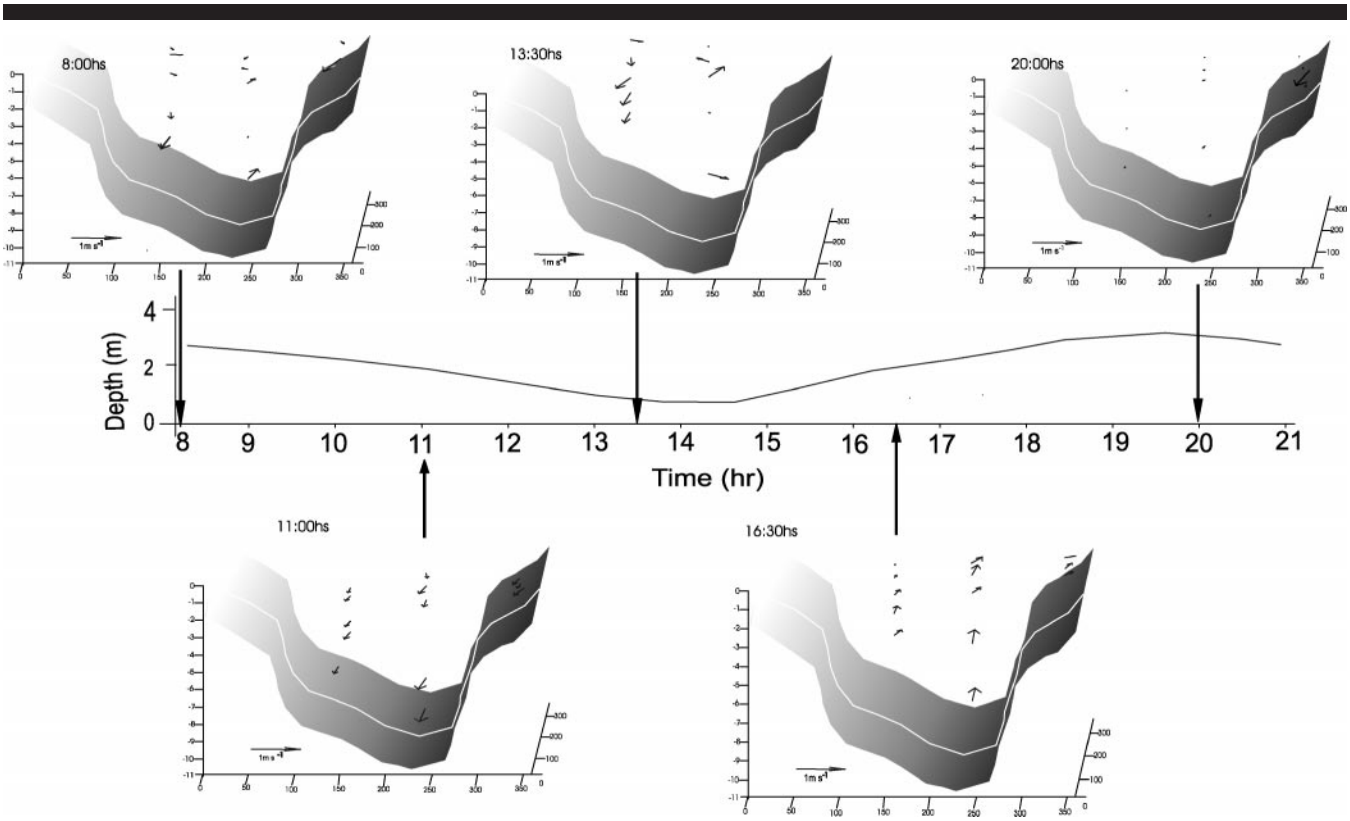

Figure 10. Pattern residual flow over the cross section.

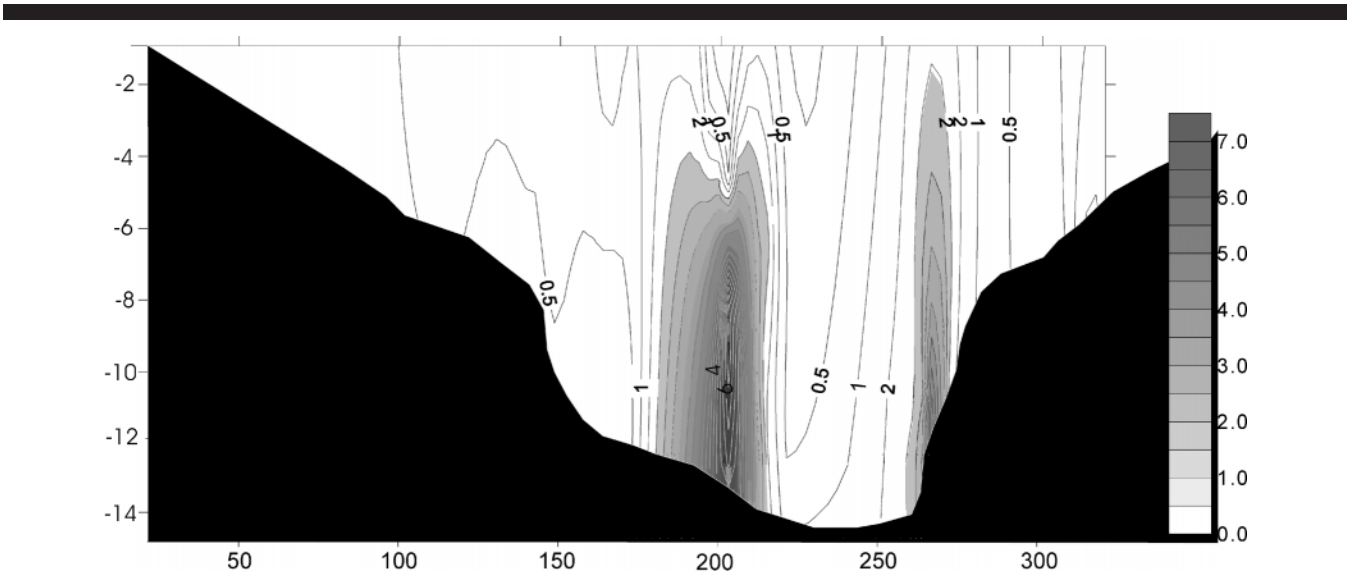

Figure 11. Vertical distribution of momentum flux along the cross section.

LITERATURE CITED

ASHLEY, G.M., 1990. Classification of large-scale subaqueous bedforms: a new look at an old problem. *Journal of Sedimentary Petrology,* 60, 160–172.

ALIOTTA, S. and PERILLO, G.M.E., 1987. A sand wave field in the entrance to Bahia Blanca Estuary, Argentina. *Marine Geology,* 76, 1–14.

BEST, J.L. and REID, I., 1984. Separation zone at open channel junctions. *Journal of Hydraulic Engineering* ASCE, 110, 1588–1594.

BEST, J.L., 1987. Flow dynamics at river channel confluences: implications for sediment transport and bed morphology. *Fluvial Sedimentology,* 39, 27–35.

BEST, J.L. and ROY, A.G., 1991. Mixing-layer distortion at the confluence of channels of different depth. *Nature,* 350, 411–413.

DYER, K.R. and NEW, A.L., 1986. Intermittency in estuarine mixing. *In*: WOLFE, D.A. (ed.) *Estuarine variability.* New York: Academic Press.

FISCHER, H.B.; LIST, E.J.; KOH, R.C.Y.; IMBERGER, J., and BROOKS, N.H., 1979. *Mixing in inland and coastal waters.* New York: Academic Press.

GINSBERG, S., 1993. Evolución Geomorfológica de los canales de marea del estuario de Bahía Blanca. Tesis Doctoral. Departamento de Geología. Universidad Nacional del Sur. 180 pp.

GINSBERG, S. and PERILLO, G.M.E., 1999. Deep- scour holes at tidal channel junctions, Bahía Blanca Estuary, Argentina. *Marine Geology,* 160, 171–182.

GÓMEZ, E.A.; GINSBERG, S., and PERILLO, G.M.E., 1996. Geomorfología y sedimentología de la zona interior del Canal Principal del Estuario de Bahía Blanca. *Asociación Argentina Sedimentología Revista,* 3–2, 55–61.

KJERFVE, B.; SHAO, CH., and STAPOR, F., 1979. Formation of deep scour holes at the junction of tidal creeks: an hypothesis. *Marine Geology,* 33, 9–14.

MOSLEY, M.P., 1982. Scour depths in branch channel confluences, Ohau River, Otago, New Zealand. *Proceedings of New Zealand Institute of Professional Engineers,* 9, 17–24.

NUNES, R.A. and SIMPSON, J.H., 1985. Axial convergence in a well mixed estuary. *Estuarine, Coastal and Shelf Science,* 20, 637–649.

OKUBO, A., 1973. Effect of shoreline irregularities on streamwise dispersion in estuaries and other embayments. *Netherlands Journal of Sea Research,* 6, 213–224.

PÉREZ, D.E. and PERILLO, G.M.E., 1998. Residual fluxes of mass, salt, and suspended sediment through a section of the Bahia Blanca Estuary. *Geoacta,* 23, 51–65.

PERILLO, G.M.E.; ARANGO, J.M., and PICCOLO, M.C., 1987. Parámetros fisicos del estuario de Bahía Blanca. Instituto Argentino de Oceanografía, *Technical Report.* 250pp.

PERILLO, G.M.E.; ARANGO, J.M.; PICCOLO, M.C., and SEQUEIRA, M.E., 1987. Hidrografía y circulación del estuario de Bahia Blanca en condiciones de Baja descarga. *En Actas 2 Congreso Latinoamericano de Ciencias del Mar.* Perú.

PERILLO, G.M.E. and SEQUEIRA, M.E., 1989. Geomorphologic and sediment transport characteristics of the middle reach of the Bahia Blanca Estuary (Argentina). *Journal Geophysical Research,* 94, 14351–14362.

PERILLO, G.M.E. and PICCOLO, M.C., 1991. Tidal response in the Bahia Blanca Estuary. *Journal Coastal Research,* 7, 437–452.

PERILLO, G.M.E. and PICCOLO, M.C., 1991. An interpolation method for estuarine and oceanographic data. *Computer & Geosciences,* 17, 813–820.

PERILLO, G.M.E. and PICCOLO, M.C., 1993. Methodology to study estuarine cross sections *Revista Geofisica,* 38, 189–206.

PERILLO, G.M.E. and PICCOLO, M.C., 1998. Importance of grid-cell area in estimation of residual fluxes. *Estuaries,* 21(1), 14–28.

PERILLO, G.M.E and PICCOLO, M.C., 1999. Geomorphologic and Physical characteristics of Bahia Blanca Estuary, Argentina. *In: Estuaries of South America: their geomorphology and dynamics. Environmental sciences series.* Berlin: Springer-Verlag.

PERILLO, G.M.E.; PIERINI, J.O.; PÉREZ, D.E., and PICCOLO, M.C., 2002. Suspended Sediment Fluxes in the Middle Reach of the Bahía Blanca Estuary, Argentina. *In:* FITZGERALD, D. and KNIGHT, J. (eds.). *Morphodynamics and Sedimentary Evolution of Estuaries.* Kluwer, Amsterdam: Kluwer.

PICCOLO, M.C. and PERILLO, G.M.E., 1990. Physical characteristics of the Bahia Blanca Estuary (Argentina) *Estuarine Coastal Shelf,* 31, 303–317.

PICCOLO, M.C.; PERILLO, G.M.E., and ARANGO, J.M., 1987. Hidrografia del estuario de Bahia Blanca, Argentina *Revista Geofísica,* 26, 75–89.

RATTRAY, M. and DWORSKI, J.G., 1980. Comparison of methods for analysis of the transverse and vertical circulation contributions to the longitudinal advective salt flux in estuaries. *Estuarine and Coastal Marine Science,* 2, 515–536.

ROY, A.G. and DE SERRES, B., 1989. Morphologie du lit et dynamique des confluents de cours d'eau. *Bulletin de la Société Géographie du Liegè,* 25, 113–127.

TURRELL, W.R.; BROWN, J., and SIMPSON, J.H., 1996. Salt intrusion and secondary flow in a shallow, well mixed estuary. *Estuarine, Coastal and Shelf Science,* 42, 153–169.

UNCLES, R.J. and JORDAN, M.B., 1979. Residual fluxes of water and salt at two stations in the sever estuary. *Estuarine, Coastal and Shelf Science,* 9, 287–302.

UNCLES, R.J.; ELLIOT, R.C.A., and WESTON, S.A., 1985. Dispersion of salt and suspended sediments in a partly mixed estuary. *Estuaries,* 3, 256–269.

WARNER, J.; SCHOELLHAMER, D.; BURAU, J., and SCHLADOW, G., 2002. Effects of tidal current phase at the junction of two straits. *Continental Shelf Research,* 22, 1629–1642.